JOURNAL OF FORENSIC SCIENCES

J Forensic Sci, May 2012, Vol. 57, No. 3
doi: 10.1111/j.1556-4029.2011.02036.x
Available online at: onlinelibrary.wiley.com

TECHNICAL NOTE

PATHOLOGY/BIOLOGY

Yong Ke,[1,2] *Ph.D.; Yang Li,*[1] *Ph.D.; and Zhen-Yuan Wang,*[1] *Ph.D.*

The Changes of Fourier Transform Infrared Spectrum in Rat Brain*

ABSTRACT: Estimation of the time since death (postmortem interval [PMI]) is one of the most difficult problems in forensic investigations, and many methods currently are utilized to estimate the PMI. The goal of this study was to investigate the changes of attenuated total reflection-Fourier transform infrared (ATR-FTIR) spectra of rat brain from postmortem time 0–144 h. The intensity ratios of major absorbance bands were examined (I_{1066}/I_{1392}, I_{1168}/I_{1392}, I_{1234}/I_{1454}, I_{1301}/I_{1392}, I_{1647}/I_{2956}, I_{2921}/I_{2850}, and I_{1647}/I_{1539}). The spectra of rat brain displayed prominent changes with increasing PMI. The band at 2871 and 1737 per cm became weak with the time increasing and even disappeared at postmortem 96 and 72 h, respectively. A close linear correlation was shown between the relative absorption intensity and the PMI, and the I_{1234}/I_{1454} offered a stronger correlation (r = 0.973). Our results indicate that ATR-FTIR spectroscopy may be a useful technique for estimating the PMI.

KEYWORDS: forensic science, postmortem interval, attenuated total reflection, fourier transform infrared spectroscopy, spectroscopy, linear regression

In daily forensic casework, estimation of the postmortem interval (PMI) is a major task. Estimation of PMI is extremely important in criminal, civil, and forensic investigations. An accurate determination of the PMI can help reconstruct a crime scene, differentiate between homicide and suicide, and pinpoint a suspect, etc.

Many methods have been attempted to accurately determine the PMI. These include examination of external physical characteristics of the body, chemical changes in body fluids, stomach contents and cadaveric temperatures (1–6), and analysis of potassium concentration in vitreous humor (7–9) and postmortem protein degradation within different tissues (10,11). In addition, some researchers have been focused on the degradation of nucleic acid including DNA and RNA (12,13). Despite the number of papers, a laboratory method for PMI determination has not been widely accepted or used in practical application. It remains a challenge for forensic scholars to look for simpler and more efficient methods to determine PMI.

Attenuated total reflection-Fourier transform infrared (ATR-FTIR) spectroscopy is one of the most powerful methods for recording IR spectra of biological materials in general. It is fast and yields a strong signal with only a few micrograms of sample because of the penetration depth of IR light in the sample for ATR measurements is independent of sample thickness. One of the key advantages of ATR-FTIR spectroscopy is that it requires minimal or no sample preparation prior to spectral measurements. In recent years, the quantitative analysis using ATR-FTIR spectroscopy has been used in many scientific fields, such as the quantification organic functional groups in ambient aerosols, the structure of leather material, the diagnosis of cancers, and other disorders (14–20). The ATR-FTIR spectroscopy does not require sample preparation or reagents as opposed to other biomolecular methods that may influence the chemical reaction within the postmortem tissues.

In the present study, we investigated the postmortem changes on an experimental animal model. The rat brain was investigated by detecting the different functional groups using ATR-FTIR spectroscopy. The correlation between the relative absorption intensity and the PMI was investigated using linear regression analyses based on ATR-FTIR data, which to our knowledge, has been reported rarely previously.

Materials and Methods

Animal Specimens

Male Sprague–Dawley rats (n = 10, 240–260 g) provided by the Animal Center of Xi'an Jiaotong University were killed by cervical dislocation, and the cadavers were kept in a controlled environment chamber set at 20(±2)°C. The brain were subsampled from the same rat at time 0, 12, 24, 48, 72, 96, 120, and 144 h (eight readings in each of 10 rats; n = 80). The tissues were placed into 2.5-mL cylindrical tubes and frozen immediately in liquid nitrogen. All of the animal experiments in the present study were performed in accordance with the principles for the Care and Use of Laboratory Animal Committee of Xi'an Jiaotong University.

ATR-FTIR Preparation

Before each measurement, the ATR crystal was carefully washed with acetone. The brain sample deposited on the ZnSe substrate directly is pressed tightly and monitored by the ATR-FTIR spectra.

[1]Department of Forensic Medicine, Xi'an Jiaotong University School of Medicine, Xi'an, P. R. China.
[2]Chongqing Public Security Bureau, Chongqing, P. R. China.
*Funded by the Council of National Natural Science Foundation of China (No. 81072509) and the Shanghai Key Laboratory of Forensic Medicine Fund (No. KF0905).

Received 29 Dec. 2010; and in revised form 1 Apr. 2011; accepted 16 Apr. 2011.

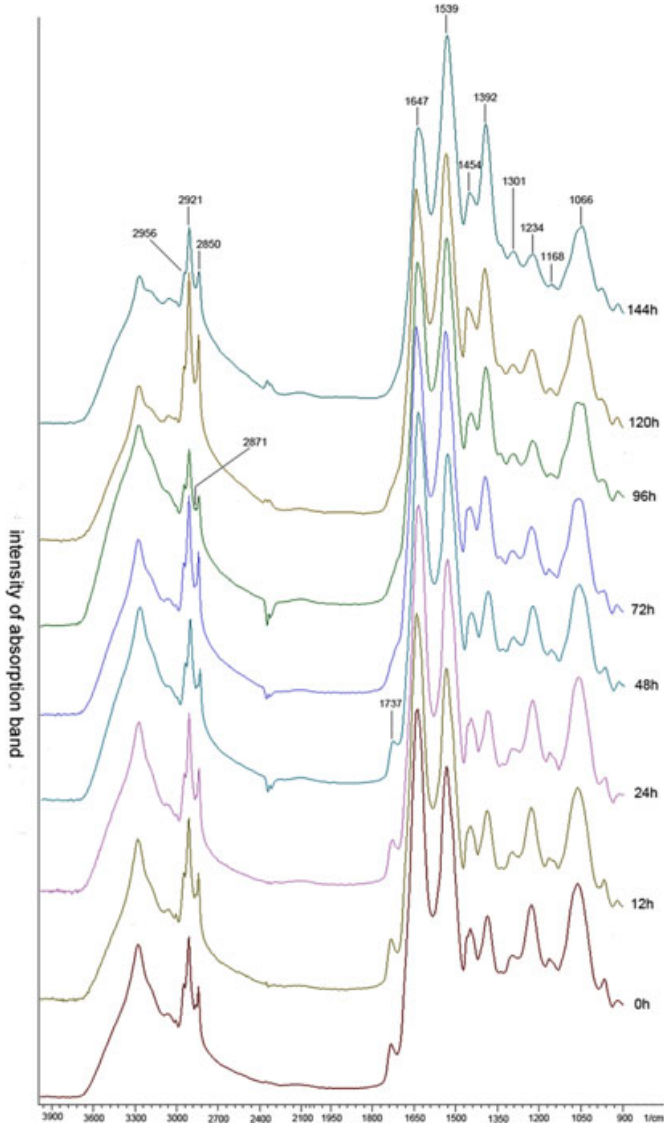

FIG. 1—*The original attenuated total reflection-Fourier transform infrared spectra in rat brain at 0–144 h postmortem.*

Spectra Measurement

The ATR-FTIR spectra were recorded quantitatively at room temperature in the range 4000–900 per cm on a Shimadzu 8400 S spectrometer equipped with ZnSe ATR device (45 entrance face) flat crystal (Shimadzu Corporation, Kyoto, Japan). Interferograms were averaged for 32 scans at 4 per cm resolution. IR solution 1.10 software (Shimadzu Corporation) was used for analysis of the FTIR spectra and for recording the data from the spectra.

Statistical Analysis

Ratios of different wavelength intensities were analyzed, so that a peak that varies with PMI is normalized by a peak that does not vary. The experimental replicates were averaged, and the mean value ± SD was calculated for each time point. Linear regression analysis between band intensity and PMI was performed and yielded the equations ($Y = Ax + B$) with a correlation coefficient (r). The p-values of <0.05 were considered statistically significant. All statistical analysis of the data was performed by using SPSS 13.0 software (SPSS Inc., Chicago, IL). Absorption bands were selected as variable or constant with respect to time and pair ratios chosen.

Results and Discussion

The intensity of the absorption bands is directly related to the concentration of the molecules (21–24). Eight complete FTIR spectra at different postmortem times showed the intensity changes of the major bands in Fig. 1. The assignment of IR absorption bands to various functional groups of some biochemical components are shown in Table 1.

As shown in Fig. 1, the absorption bands at 2871 per cm and 1737 per cm became weak with the increase in time and even disappeared at postmortem 96 h and 72 h, respectively. It is well known that the molecule contents decreased gradually as the degradation of the tissue after the organism died. This could be used as a marker to estimate the PMI. In Fig. 2*C*, the I_{2921}/I_{2850} ratios showed decrease from 0 to 144 h postmortem. Our results show that the ratios of C–H stretching bands decreased significantly at postmortem. We thought it is because of the hydrolysis of lysosomal enzyme, which is similar to the degradation of proteins and nucleic acids.

In Fig. 1, we can see that the amide II band is greater than the amide I band at the later time points, while this result was different with the former reports (15,35–38). In the former reports, the amide II band is lower than the amide I band obviously at the later time points. We thought the difference was caused by the influence of water. The band at 1647 per cm also belongs to the H-O-H variable-angle vibration of water (39,40). In the former studies, the KBr pellet method was used, and the tissue was freeze-dried in vacuo, which can avoid the influence of water. Figure 2*A* shows

TABLE 1—*Major attenuated total reflection-Fourier transform infrared spectra peak and assignments (21–34).*

Wave Number (cm^{-1})	Band Assignments	Functional Group
2956	CH_3 asymmetric stretching	Lipid
2921	CH_2 asymmetric stretching	Lipid
2871	CH_3 symmetric stretching	Lipid
2850	CH_2 symmetric stretching	Lipid
1737	C = O stretching vibration	Lipid
1647	C = O stretching	Amide I band of tissue and cell proteins
1539	N–H bending, C–N stretching	Amide II band of tissue proteins
1454	CH_2 bending, CH_3 symmetric bending	Mainly lipids and methyl groups in proteins
1392	CH_3 asymmetric Bending, COO^- symmetric stretching	Methyl groups in proteins, fatty acids, and amino acids
1301	C-OH bending vibration	Uncertain
1234	PO_2^- asymmetric stretching	Nucleic acid
1168	C-O(H) stretching	Serine, threonine, and tyrosine in cell proteins
1066	PO_2^- symmetric stretching	Nucleic acid

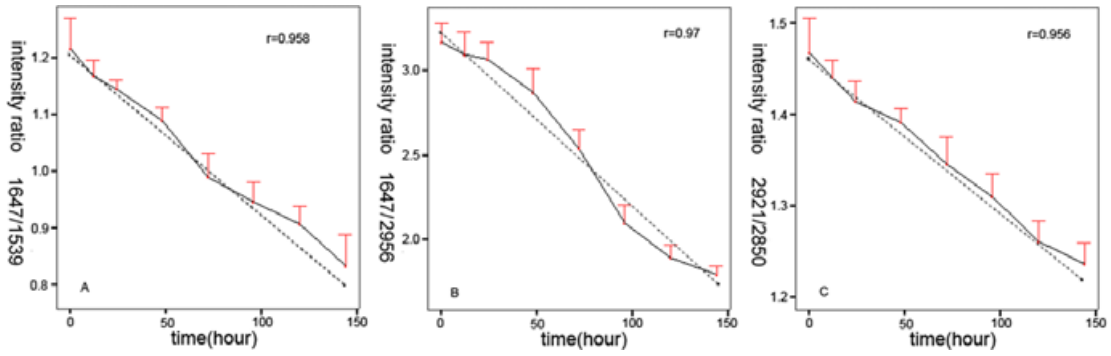

FIG. 2—*The intensity ratio of the bands (A) I_{1647}/I_{1539}, (B) I_{1647}/I_{2956}, and (C) I_{2921}/I_{2850} at each time point postmortem. The dotted line (- - -) presented linear relationship between intensity ratio and postmortem interval.*

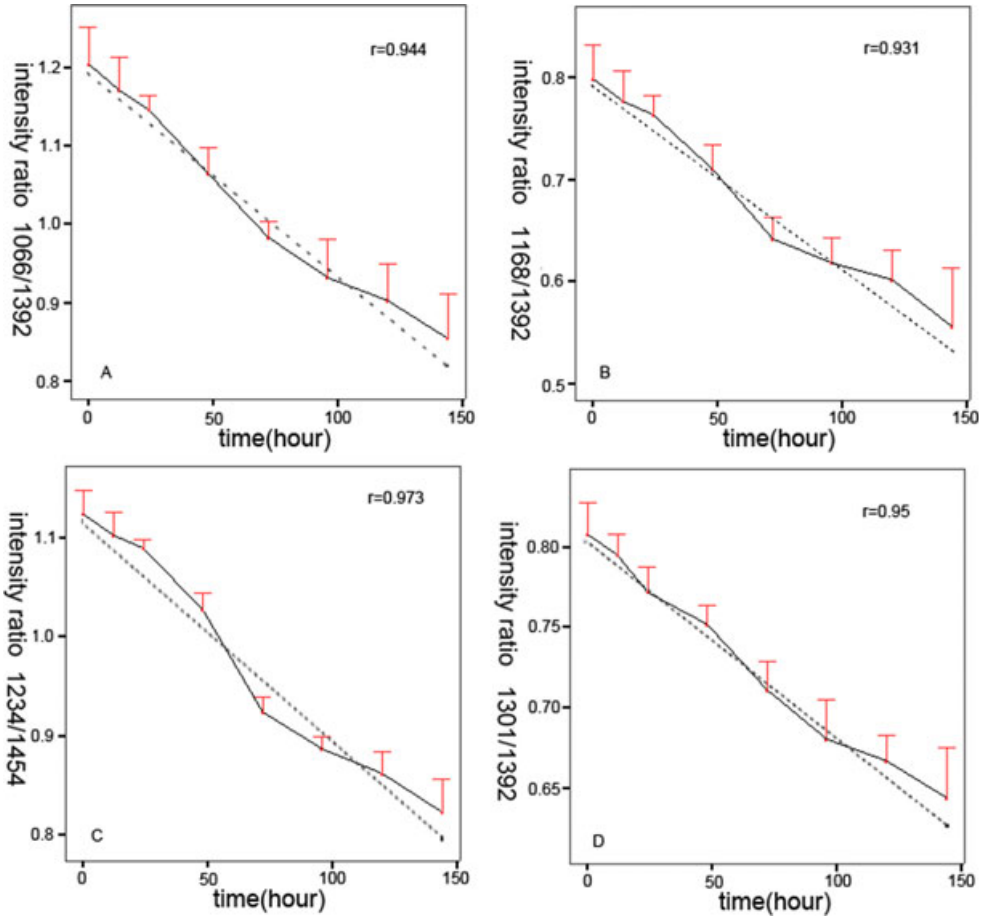

FIG. 3—*The intensity ratio of the bands (A) I_{1066}/I_{1392}, (B) I_{1168}/I_{1392}, (C) I_{1234}/I_{1454}, (D) I_{1301}/I_{1392} at each time point postmortem. The dotted line (- - -) presented linear relationship between intensity ratio and postmortem interval.*

TABLE 2—*The linear regression equations of different ratios of absorption intensity.*

Numbers	Linear Regression Equation	x Assignment	Correlation Coefficient, r	Significance, p
1	$Y = -355.576\ x + 431.637$	I_{1066}/I_{1392}	0.944	<0.001
2	$Y = -423.528\ x + 480.095$	I_{1234}/I_{1454}	0.973	<0.001
3	$Y = -509.689\ x + 413.268$	I_{1168}/I_{1392}	0.931	<0.001
4	$Y = -771.956\ x + 626.970$	I_{1301}/I_{1392}	0.950	<0.001
5	$Y = -353.141\ x + 430.000$	I_{1647}/I_{1539}	0.958	<0.001
6	$Y = -572.794\ x + 842.240$	I_{2921}/I_{2850}	0.956	<0.001
7	$Y = -88.283\ x + 291.842$	I_{1647}/I_{2956}	0.970	<0.001

Y, represents postmortem interval (hours); x, represents ratio of absorption intensity; I, intensity of absorbance band.

that the ratio of amide I and amide II intensity decreased postmortem.

The more precise changes of 1454, 1392, 1301, 1234, 1168, and 1066 using the intensity bands ratios were displayed in Fig. 3*A–D*. As demonstrated, the I_{1066}/I_{1392}, I_{1168}/I_{1392}, I_{1234}/I_{1454}, and I_{1301}/I_{1392} ratios showed dramatic decrease with increasing time since death. It was found that the postmortem DNA degradation occurs in porcine skeletal muscle from 3 to 56 h using single cell gel electrophoresis. However, DNA in porcine kidney cannot be detected possibly due to its autolysis (41). Quantification of mRNA and DNA degradation is closely correlated with the PMI in autopsy cases (12,13).

Furthermore, the correlations between the band intensity ratios and PMI were analyzed. The linear regression equations of the different intensity ratios were demonstrated in Table 2.

As shown in Table 2, linear regression analysis showed strong correlations between the intensity ratios and the time since death. Among all the ratios, the I_{1234}/I_{1454} ($r = 0.973$), I_{1647}/I_{2956} ($r = 0.970$), I_{2921}/I_{2850} ($r = 0.956$), and I_{1647}/I_{1539} ratios ($r = 0.958$) showed strongest decreasing linear correlations with the PMI. Our results suggest that the FTIR spectroscopy can be used to monitor the degradation of biomolecules up to 144 h with high efficiency.

Conclusion

Our results indicate that FTIR spectroscopic analysis can monitor the postmortem metabolic changes at molecular level from 0 to 144 h postmortem in rat brain. The absorption intensity ratios show close linear correlations against PMI. Additionally, FTIR technique does not require sample preparation or reagents as compared with other biomolecular methods. Therefore, it has a less influence on the chemical changes within the tissues postmortem. Compared with other classical methods, FTIR spectroscopy may be a great tool for estimating PMI in the forensic investigations.

References

1. Baccino E, Cattaneo C, Jouineau C, Poudoulec J, Martrille L. Cooling rates of the ear and brain in pig heads submerged in water: implications for postmortem interval estimation of cadavers found in still water. Am J Forensic Med Pathol 2007;28(1):80–5.
2. Henssge C, Althaus L, Bolt J, Freislederer A, Haffner HT, Henssge CA, et al. Experiences with a compound method for estimating the time since death. I. Rectal temperature nomogram for time since death. Int J Legal Med 2000;113(6):303–19.
3. Henssge C, Madea B. Estimation of the time since death in the early post-mortem period. Forensic Sci Int 2004;3:167–75.
4. Madea B, Kreuser C, Banaschak S. Postmortem biochemical examination of synovial fluid—a preliminary study. Forensic Sci Int 2001;118(1):29–35.
5. Honjyo K, Yonemitsu K, Tsunenari S. Estimation of early postmortem intervals by a multiple regression analysis using rectal temperature and non-temperature based postmortem changes. J Clinical Forensic Med 2005;12(5):249–53.
6. Henssge C, Madea B. Estimation of the time since death. Forensic Sci Int 2007;3:182–4.
7. James RA, Hoadley PA, Sampson BG. Determination of postmortem interval by sampling vitreous humour. Am J Forensic Med Pathol 1997;18(2):158–62.
8. Munoz JI, Suarez-Penaranda JM, Otero XL, Rodriguez-Calvo MS, Costas E, Miguens X, et al. A new perspective in the estimation of postmortem interval (PMI) based on vitreous. J Forensic Sci 2001;46(2):209–14.
9. Keller LP, Bajt S, Baratta GA, Borg J, Bradley JP, Brownlee DE, et al. Infrared spectroscopy of comet 81P/Wild 2 samples returned by Stardust. Science 2006;314(5806):1728–31.
10. Sabucedo AJ, Furton KG. Estimation of postmortem interval using the protein marker cardiac Troponin I. Forensic Sci Int 2003;134(1):11–6.
11. Kang S, Kassam N, Gauthier ML, O'Day DH. Post-mortem changes in calmodulin binding proteins in muscle and lung. Forensic Sci Int 2003;3:140–7.
12. Cina SJ. Flow cytometric evaluation of DNA degradation: a predictor of postmortem interval? Am J Forensic Med Pathol 1994;15(4):300–2.
13. Bauer M, Gramlich I, Polzin S, Patzelt D. Quantification of mRNA degradation as possible indicator of postmortem interval—a pilot study. Legal Med 2003;5(4):220–7.
14. Coury C, Dillner AM. A method to quantify organic functional groups and inorganic compounds in ambient aerosols using attenuated total reflectance FTIR spectroscopy and multivariate chemometric techniques. Atmos Environ 2008;42(23):5923–32.
15. Huang P, Tian W, Tuo Y, Wang Z, Yang G. Estimation of postmortem interval in rat liver and spleen using fourier transform infrared spectroscopy. Spectrosc Lett 2009;42(2):108–16.
16. Boncheva M, Damien F, Normand V. Molecular organization of the lipid matrix in intact stratum corneum using ATR-FTIR spectroscopy. Biochim Biophys Acta 2008;1778(5):1344–55.
17. Vigano C, Manciu L, Buyse F, Goormaghtigh E, Ruysschaert JM. Attenuated total reflection IR spectroscopy as a tool to investigate the structure, orientation and tertiary structure changes in peptides and membrane proteins. Biopolymers 2000;55(5):373–80.
18. Laugel C, Yagoubi N, Baillet A. ATR-FTIR spectroscopy: a chemometric approach for studying the lipid organisation of the stratum corneum. Chem Phys Lipids 2005;135(1):55–68.
19. Ricci C, Chan KL, Kazarian SG. Combining the tape-lift method and Fourier transform infrared spectroscopic imaging for forensic applications. Appl Spectrosc 2006;60(9):1013–21.
20. van de Weert M, Haris PI, Hennink WE, Crommelin DJA. Fourier transform infrared spectrometric analysis of protein conformation: effect of sampling method and stress factors. Anal Biochem 2001;297(2):160–9.
21. Rigas B, Morgello S, Goldman IS, Wong PT. Human colorectal cancers display abnormal Fourier-transform infrared spectra. Proc Natl Acad Sci USA 1990;87(20):8140–4.
22. Cohenford MA. Cytologically normal cells from neoplastic cervical samples display extensive structural abnormalities on IR spectroscopy: implications for tumor biology. Proc Natl Acad Sci USA 1998;95(26):15327–32.
23. Cakmak G, Togan I, Severcan F. 17 [beta]-Estradiol induced compositional, structural and functional changes in rainbow trout liver, revealed by FT-IR spectroscopy: a comparative study with nonylphenol. Aquat Toxicol 2006;77(1):53–63.
24. Cakmak G, Togan I, Uguz C, Severcan F. FT-IR spectroscopic analysis of rainbow trout liver exposed to nonylphenol. Appl Spectrosc 2003;57(7):835–41.
25. Jackson M, Choo LP, Watson PH, Halliday WC, Mantsch HH. Beware of connective tissue proteins: assignment and implications of collagen absorptions in infrared spectra of human tissues. Biochim Biophys Acta 1995;1270(1):1–6.
26. Wong PT, Wong RK, Caputo TA, Godwin TA, Rigas B. Infrared spectroscopy of exfoliated human cervical cells: evidence of extensive structural changes during carcinogenesis. Proc Natl Acad Sci USA 1991;88(24):10988–92.
27. Stuart BH. Infrared spectroscopy: fundamentals and applications. New York, NY: John Wiley, 2004.
28. Gaudenzi S, Pozzi D, Toroa P, Silvestrib I, Morroneb S, Castellanoc AC. Cell apoptosis specific marker found by Fourier transform infrared spectroscopy. Spectroscopy 2004;18(3):415–22.
29. Wood BR, Quinn MA, Tait B, Ashdown M, Hislop T, Romeo M, et al. FTIR microspectroscopic study of cell types and potential confounding variables in screening for cervical malignancies. Biospectroscopy 1998;4(2):75–91.
30. Wong PTT, Lacelle S, Fung MFK, Senterman M, Mikhael NZ. Characterization of exfoliated cells and tissues from human endocervix and ectocervix by FTIR and ATR/FTIR spectroscopy. Biospectroscopy 1995;1(5):357–64.
31. Severcan F, Kaptan N, Turanb B. Fourier transform infrared spectroscopic studies of diabetic rat heart crude membranes. Spectroscopy 2003;17(2):569–77.
32. Toyran N, Lasch P, Naumann D, Turan B, Severcan F. Early alterations in myocardia and vessels of the diabetic rat heart: an FTIR microspectroscopic study. Biochem J 2006;397(3):427–36.
33. Severcan F, Gorgulu G, Gorgulu ST, Guray T. Rapid monitoring of diabetes-induced lipid peroxidation by Fourier transform infrared spectroscopy: evidence from rat liver microsomal membranes. Anal Biochem 2005;339(1):36–40.

34. Guan XH, Chen GH, Shang C. ATR-FTIR and XPS study on the structure of complexes formed upon the adsorption of simple organic acids on aluminum hydroxide. J Environ Sci (China) 2007;19(4): 438–43.
35. Huang P, Ke Y, Lu Q, Xin B, Fan S, Yang G, et al. Analysis of postmortem metabolic changes in rat kidney cortex using Fourier transform infrared spectroscopy. Spectroscopy 2008;22(1):21–31.
36. Tuo Y, Huang P, Ke Y, Fan S, Lu Q, Xin B, et al. Attenuated total reflection fourier transform infrared spectroscopic investigation of the postmortem metabolic process in rat and human kidney cortex. Appl Spectrosc 2010;64(3):268–74.
37. Ping H, Ya TUO, Zhen-yuan W. Review on estimation of postmortem interval using FTIR spectroscopy. J Forensic Med 2010;26(03): 198–201.
38. Ke Y, Wang SW, Lu QY, Huang P, Xing B, Wang ZY. The correlation between postmortem interval and Fourier transform infrared spectra in rat's brain. Spectrosc Spect Anal 2008;28(11):2545–9.
39. Massaro S, Zlateva T, Torre V, Quaroni L. Detection of molecular processes in the intact retina by ATR-FTIR spectromicroscopy. Anal Bioanal Chem 2008;390(1):317–22.
40. Li QB, Sun XJ, Xu YZ, Yang LM, Zhang YF, Weng SF, et al. Use of Fourier-transform infrared spectroscopy to rapidly diagnose gastric endoscopic biopsies. World J Gastroenterol 2005;11(25):3842–5.
41. Johnson LA, Ferris JAJ. Analysis of postmortem DNA degradation by single-cell gel electrophoresis. Forensic Sci Int 2002;126(1):43–7.

Additional information and reprint requests:
Zhen-Yuan Wang, Ph.D.
Department of Forensic Medicine
Xi'an Jiaotong University School of Medicine
Xi'an, P. R.
China
E-mail: wzy218@mail.xjtu.edu.cn